Electronic Supplementary Information

Dynamic strain in gold nanoparticle supported graphene induced by focused laser irradiation

*András Pálinkás[1,2], Péter Kun[1,2], Antal A. Koós[1,2], Zoltán Osváth[1,2,]**

[1]Institute of Technical Physics and Materials Science, MFA, Centre for Energy Research, Hungarian Academy of Sciences, 1525 Budapest, P.O. Box 49, Hungary

[2]Korea-Hungary Joint Laboratory for Nanosciences (KHJLN), 1525 Budapest, P.O. Box 49, Hungary

1. Effect of laser annealing on the local graphene morphology

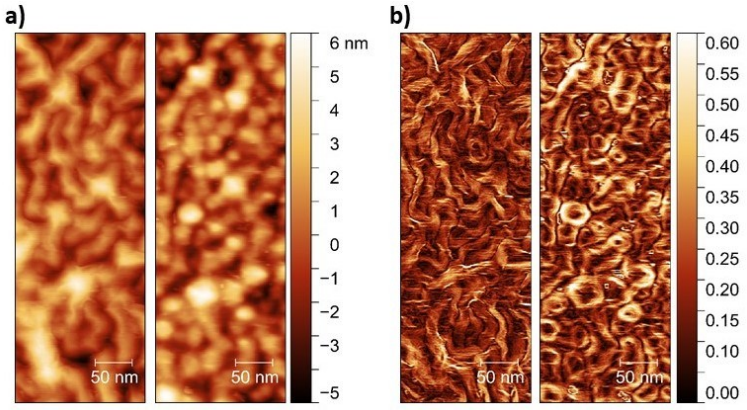

Figure S1. *(a) AFM images of graphene covered gold nanoparticles. The same area is shown before (left) and after (right) laser annealing. (b) Calculated graphene slopes* $\left(\frac{dz}{dx},\frac{dz}{dy}\right)$*, where the z values correspond to the measured heights from a), accordingly.*

Figure S1-a shows the AFM images of the same area of graphene/gold nanoparticles before (left) and after (right) high intensity laser irradiation. Note that before laser annealing, graphene has elongated ripples, while after annealing its corrugation is determined by the underlying nanoparticles. Figure S1-b shows the spatial distribution of local graphene slopes $\left(\frac{dz}{dx},\frac{dz}{dy}\right)$, where the *z* values correspond to the measured heights from Fig. S1-a. The elongated

shapes are observed in the calculated slopes as well (left panel), while after laser irradiation the slopes are more circular, centred at individual NPs (right panel). Notice that these circular shapes are brighter, denoting increased slopes. We infer that the graphene-gold interaction is stronger in this close-to-conformal geometry. Hence, when further laser annealing occurs, the nanoparticles expand and induce tensile strain in the graphene parts they support, according to the Equation 2 in the main text.

2. Scanning electron microscopy (SEM) of graphene/gold nanoparticle hybrids

The laser annealed areas could be discerned from the as-deposited gold layer during SEM investigations as well. For example, the upper-left area of Figure S2-a shows a part from a (graphene covered) laser annealed region, the boundaries of which are marked by yellow dash-dotted lines. Furthermore, Figure S2-c shows an entire 5×5 μm^2 laser annealed area. Here, a tilt angle of 60° was used. The Raman spectroscopy data presented in Fig. 4 of the main text were measured on this area. Figure S2-b and S2-d show higher magnification SEM images.

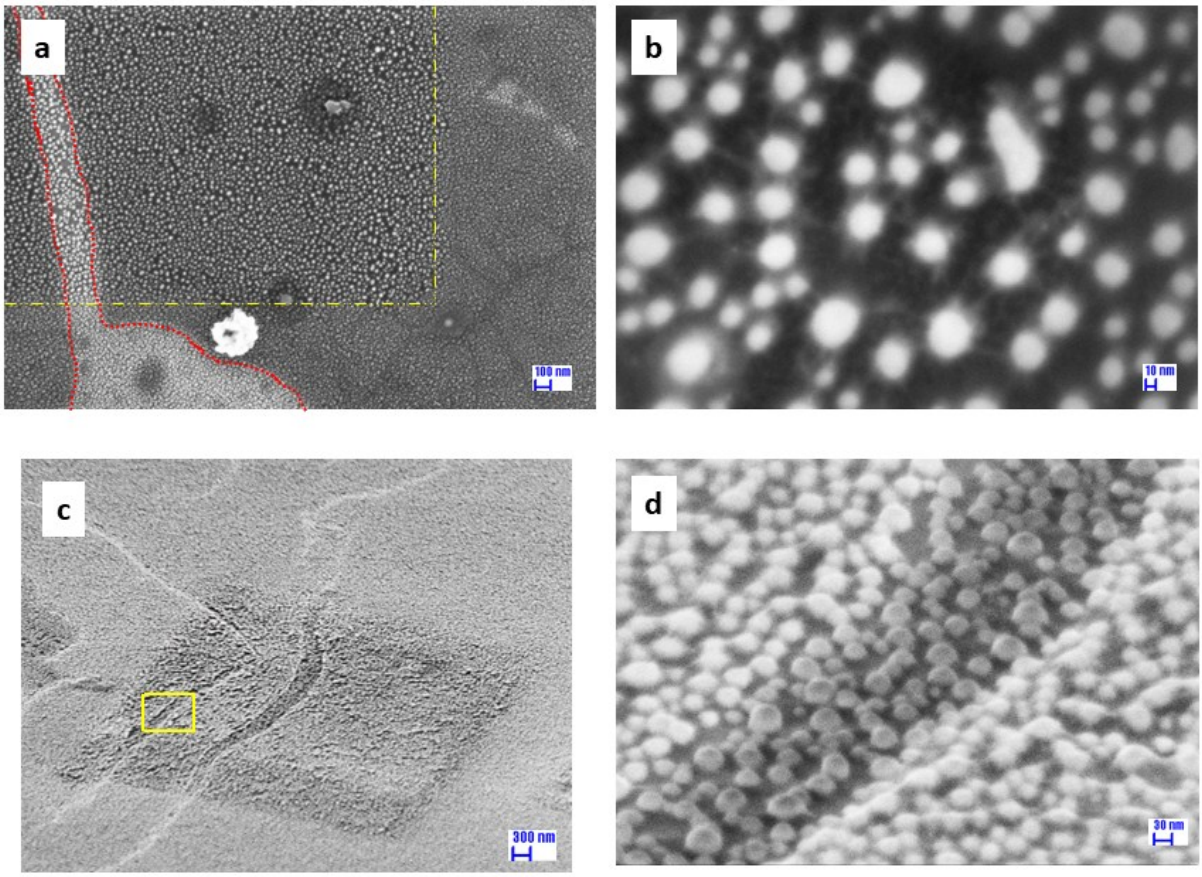

Figure S2. *SEM images of graphene covered gold nanoparticles acquired with a LEO 1540 XB operating at 3kV. (a) The upper-left area delimited with yellow dash-dotted lines was annealed by a focused laser beam of 6 mW. Graphene edges are marked with red dotted lines. (b) High magnification SEM image of a laser-annealed, graphene-covered area. Graphene "bridges" are observed between neighbouring nanoparticles. (c) SEM image of the laser annealed area corresponding to Fig. 4 in the main text. Two graphene cracks traverses the annealed area. A high magnification image of the region marked with yellow rectangle is shown in (d). Here, the darker, diagonal stripe corresponds to a graphene crack, where bare gold nanoparticles are observed, while the light contrasted areas around this stripe show graphene covered*

nanoparticles. Fig. c) and d) were acquired by tilting the electron beam 60° relative to the surface normal.

3. Analysis of the full widths at half maximum (FWHM) of Raman 2D peaks

The doping of graphene modifies not only the Raman peak positions, but their width as well[i]. Increased doping level will result in broadened 2D peak[ii-iii]. Since not only the doping, but also the increasing temperature has a broadening effect on the Raman peaks[iv,v], here we analyse only the results obtained with low laser power (0.6 mW), in order to exclude temperature effects. The FWHM calculated from the data sets of Fig. 3a (1, 3, 5), main text (graphene on SiO_2), are shown in Figure S3.

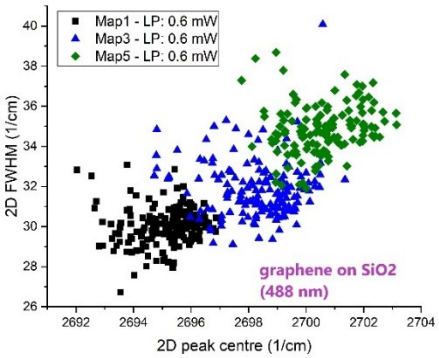

Figure S3. *FWHM of 2D Raman peaks and their spectral centre on Si/SiO_2 supported graphene, measured with 488 nm laser excitation.*

The increasing FWHM is clearly observed in the successive measurements, which is consistent with the increasing doping. Further, the 2D FWHM data sets corresponding to the successive low power measurements on gold nanoparticle supported graphene (Figure 4 in the main text) are shown in Figure S4, for excitations of 633 nm and 488 nm, respectively. In contrast to graphene on SiO_2, the different data sets are well mixed, and there is no significant shift of the FWHM distribution (apart from a few data points with the 488 nm laser). This confirms that residual doping is not induced on gold nanoparticle supported graphene.

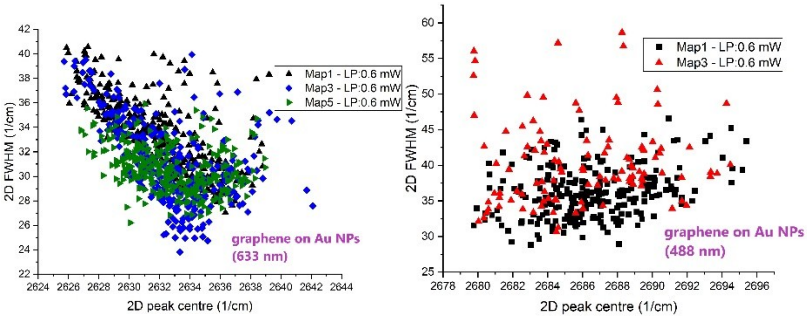

Figure S4. *FWHM of 2D Raman peaks and their position on gold nanoparticle supported graphene measured with 633 nm (left) and 488 nm (right) laser excitation.*

References

[i] A. Das, S. Pisana, B. Chakraborty, S. Piscanec, S.K. Saha, U. V. Waghmare, K.S. Novoselov, H.R. Krishnamurthy, A.K. Geim, A.C. Ferrari, A.K. Sood, Monitoring dopants by Raman scattering in an electrochemically top-gated graphene transistor, Nat. Nanotechnol. 3 (2008) 210–215. doi:10.1038/nnano.2008.67.

[ii] M. Kalbac, A. Reina-Cecco, H. Farhat, J. Kong, L. Kavan, M.S. Dresselhaus, J. Heyrovsky, The Influence of Strong Electron and Hole Doping on the Raman Intensity of Chemical Vapor-Deposition Graphene, ACS Nano. 4 (2010) 6055–6063.

[iii] A.C. Ferrari, D.M. Basko, Raman spectroscopy as a versatile tool for studying the properties of graphene, Nat. Nanotechnol. 8 (2013) 235–246. doi:10.1038/nnano.2013.46.

[iv] L.M. Malard, R.L. Moreira, D.C. Elias, F. Plentz, E.S. Alves, M. Pimenta, Thermal enhancement of chemical doping in graphene: A Raman spectroscopy study, J. Phys. Condens. Matter. 22 (2010) 334202. doi:10.1088/0953-8984/22/33/334202.

[v] J. Judek, A.P. Gertych, M. Krajewski, K. Czerniak, A. Łapińska, J. Sobieski, M. Zdrojek, Statistical analysis of the temperature dependence of the phonon properties in supported CVD graphene, Carbon N. Y. 124 (2017) 1–8. doi:10.1016/j.carbon.2017.08.029.